Visually Stressful Striped Patterns Alter Human Visual Cortical Functional Connectivity

Jie Huang [iD][1]* and David C. Zhu[1,2]

[1]Department of Radiology, Michigan State University, East Lansing, Michigan
[2]Department of Psychology, Michigan State University, East Lansing, Michigan

◆ ────────────────────── ◆

Abstract: Visually stressful striped patterns with a spatial frequency (SF) of around 3 cycles per degree (cpd) can induce perceptual illusions/distortions and visual discomfort in most people, headaches in patients with migraine, and seizures in patients with photosensitive epilepsy. Patterns with SF ∼0.3 cpd have no such effects and are not uncomfortable to look at (non-stressful). The effects of the striped patterns on visual cortical activation have been investigated, but their effects on the visual cortical network remain to be studied. A prolonged visual stimulation with stressful patterns may alter the functional connections within the visual system, and their relationship with other networks. Using resting-state fMRI, this study revealed that the functional connections within the visual system were significantly enhanced by visually stressful stimulation. The functional connectivity between V1 and other brain regions was also significantly modified. Non-stressful stimulation produced no such significant effects. More importantly, the effects outlasted the stimulation, and this applied both to those effects within and those beyond the visual cortex, suggesting that repeated prolonged visual stimulation with stressful patterns may alter functional connections of the brain and this might be utilized as a visual neuromodulation approach for treatments of visually triggered headaches in migraine patients and visually induced seizures in patients with photosensitive epilepsy. *Hum Brain Mapp 38:5474–5484, 2017.*   © 2017 **Wiley Periodicals, Inc.**

Key words: human brain; resting-state fMRI; functional connectivity; visual cortex; visual neuromodulation

◆ ────────────────────── ◆

INTRODUCTION

A striped pattern with spatial frequency (SF) of ∼3 cycles per degree (cpd) can induce perceptual illusions/distortions and visual discomfort in most people, headaches in patients with migraine, and seizures in patients with photosensitive epilepsy [Wilkins, 1995; Wilkins et al., 1984]. This pattern provokes maximal perceptual illusions and visual discomfort,

and is also most unpleasant (stressful) to look at. In contrary, a striped pattern with SF ∼ 0.3 cpd does not induce such effects and is not unpleasant at all to look at. The only difference between these stressful and non-stressful striped patterns is the spatial period. In comparison to a stressful striped pattern, a squared pattern (checkerboard) with the same SF is less aversive [Wilkins, 1995], suggesting that the visual cortex is likely to be responsible for the pattern-induced visual symptoms. This is because it is the primary visual cortical neurons but not the retinal ganglion and lateral geniculate cells which maximally respond to a long narrow rectangle of light or edge [Hubel and Wiesel, 1962, 1968].

Neurons in visual cortical areas V1 and V2 respond selectively not only to oriented long narrow rectangles of light, but also selectively to the SF of striped patterns [Foster et al., 1985]. For both V1 and V2 neurons, typical SF-selective response curves exhibit a SF-tuning feature that is maximized at an optimal SF; the response decreases markedly to SFs higher or lower than the optimal SF. The histogram of these optimal SFs distribution is, however,

dramatically different for V1 neurons and V2 neurons. The largest percentage of the V1 neurons with optimal SF is at 2.8 cpd. A contrast sensitivity study shows that the SF of the maximal sensitivity occurs at approximately 3 cpd under photopic levels of illumination (mean luminance 500 cd/m^2) [Campbell and Robson, 1968], similar to that of the maximum of the optimal SF distribution of the V1 neurons, suggesting the latter might be responsible for the former. This optimal SF distribution might also be responsible for the maximal pattern-induced perceptual illusions and visual discomfort at ~3 cpd [Huang and Cao, 2012]. The largest percentage of the V2 neurons with optimal SF is shifted to 0.75 cpd, indicating a low-pass SF-tuning in V2. This SF shift in the maximum of the histogram from 2.8 cpd in V1 to 0.75 cpd in V2 signifies the importance of the low-pass SF-tuning in normal information processing from V1 to V2.

The non-invasive blood oxygenation level dependent (BOLD) functional magnetic resonance imaging (fMRI) technique has evolved as a major neuroimaging tool for studying human brain functions at large-scale neural activity [Kwong et al., 1992; Logothetis, 2008; Ogawa et al., 1990]. In a typical fMRI study with a spatial resolution of $3 \times 3 \times 3$ mm^3, an activated voxel may contain over million neurons and its corresponding BOLD signal change measures the activity-induced change from a pooled activity of this neuron population [Logothetis, 2008]. For healthy humans, BOLD-fMRI studies showed that the maximal cortical activation is at ~3 cpd in V1, but is shifted to ~0.3 cpd in V2, consistent with the histograms of the V1 and V2 neurons, respectively [Huang et al., 2011; Singh et al., 2000]. The maximal cortical activation at ~0.3 cpd in V2 likely reflects the maximal response from the largest percentage of the V2 neurons with optimal SF 0.75 cpd. As the V1 output is the main input of V2, the smaller cortical activation at ~3 cpd in V2, however, seems to suggest an inhibitory neural response to the output of the maximal response to ~3 cpd from the largest percentage of the V1 neurons with optimal SF 2.8 cpd. If this is true, an insufficient inhibitory neural response in V2 would manifest as visual cortical hyper-response that could be responsible for pattern-induced illusions, discomfort, headaches and seizures [Huang and Cao, 2012].

Early fMRI studies demonstrated that visually triggered migraine symptoms in patients with migraine with aura are linked with visual cortical BOLD signal changes [Cao et al., 1999, 2002]. One fMRI study also elicited the source of aura-related BOLD signal changes located in extrastriate visual cortex (V3A) rather than in V1 [Hadjikhani et al., 2001]. Our early fMRI study found that the stressful striped pattern-provoked perceptual illusions in patients with migraine with aura are associated with the pattern-induced hyper-activation in primary visual cortex [Huang et al., 2003]. Our recent fMRI study on migraine showed that the maximal cortical activation was at ~3 cpd in both V1 and V2, demonstrating an insufficient inhibitory neural response to SF ~3 cpd in V2 [Huang et al., 2011]. Precision

ophthalmic tint (POT) lenses have been reported to reduce perceptual illusions, visual discomfort and migraine headaches [Wilkins et al., 1992, 2002]. Our study also showed that the POT lenses not only reduced the pattern-provoked illusions and discomfort, but also normalized the V2 activation, suggesting the POT-reduced cortical response is responsible for the POT-reduced illusions, discomfort and headaches [Huang et al., 2011].

The effects of the striped patterns on visual cortical activation have been investigated [Huang et al., 2003, 2011; Singh et al., 2000], but their effects on the visual cortical network remain to be studied. Resting-state fMRI (rs-fMRI) has been widely used to study functional connections (FC) between regions in the brain, and functionally connected areas across the visual cortex have been well recognized [Biswal et al., 1995; Yeo et al., 2011]. The effect of stressful visual stimulation on human visual cortical FC, however, remains to be investigated. Furthermore, it also remains to be investigated how to use the stressful visual stimulation to visually modulate visual cortical hyper-response for preventing visually triggered headaches. A six-week study of chronic worriers showed that the number of stressful pattern-induced illusions reported on non-headache days was significantly correlated with the total number of headaches, suggesting that greater pattern sensitivity was associated with more headaches [Nulty et al., 1987]. Furthermore, the study also found that in the 24 h prior to headache onset illusion susceptibility was enhanced. These results suggest a reduced pattern sensitivity may reduce the frequency of headaches. Stroboscopically induced seizure discharges were modified and ameliorated by repeated extinction trials, showing that it is possible to moderate and even alleviate the dysrhythmia induced by intermittent light stimulation that leads to possibilities for therapy [Forster et al., 1964]. In this study, we conducted two experiments (Exps) to investigate the effects of visual stimulation with stressful versus non-stressful striped patterns on human visual cortical FC. Exp 1 investigated the effects of stressful visual stimulation on visual cortical FC, and Exp 2 investigated the effects of non-stressful visual stimulation on visual cortical FC. Based on the results, we propose a potentially safe, comfortable, and repetitive visual stimulation paradigm to modulate visual cortical FC for prophylactic treatment in patients suffering visually triggered headaches or seizures.

METHODS AND MATERIALS

Subjects: Twelve healthy subjects (7 male and 5 female, ages from 19 to 55 with mean 28.4 ± 13.6 years) participated in Exp I, and 12 healthy subjects (7 male and 5 female, ages from 22 to 56 with mean 32.7 ± 12.2 years) participated in Exp II. (Six of them participated in both Exps I and II, and the interval between the two Exps was about one year.) There was no statistically significant difference in age between the two subject groups (two-tails t-test, $P = 0.42$). The Institutional Review Board at Michigan

State University approved the study, and written informed consent was obtained from all subjects prior to the study.
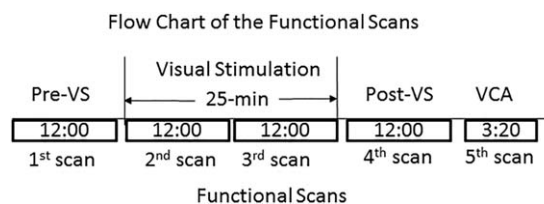
Visual Stimulation Paradigm

A visual stimulation paradigm was used to determine the effects of visual stimulation with stressful or non-stressful striped patterns on the visual cortical FC. The paradigm consists of alternating 2-sec visual stimulation on-and-off for 25 min. The stimulus was a black-and-white stressful striped pattern with SF 2.8 cpd for Exp I, but a non-stressful striped pattern with SF 0.27 cpd for Exp II. The size of visual field was 23x30 degree visual angle. The striped pattern was vertically oriented with a square-wave luminance profile (mean luminance 171.3 cd/m^2, Michelson contrast 98.3%), and remained stationary during each of the 2-sec stimulation on period. During the off period, a blank screen with the same mean luminance as the striped pattern was presented. Both the striped pattern and blank screen had a small black square fixation mark at the center of the screen, and the subjects were instructed to focus their eyes on the fixation mark during the whole scan.

Visual Cortical Activation Paradigm

A visual cortical activation paradigm was used to determine the activated voxels in the putative primary visual area V1. The paradigm comprised five alternating 20-sec visual stimulation on-and-off blocks with the stimulus with SF 2.8 cpd and blank screen used in the visual stimulation paradigm for both Exps I and II.

Image Acquisition

Functional brain images were acquired on a GE 3T Signa® HDx MR scanner (GE Healthcare, Waukesha, WI) with an 8-channel head coil using a gradient echo Echo-Planar-Imaging (EPI) pulse sequence (TE/TR = 28/2,500 ms, flip angle 80°, FOV 22 cm, matrix 64 × 64, slice thickness 3.0 mm, and spacing 0.0 mm). Thirty-eight axial slices to cover the brain were scanned, and the first four volume images were discarded. The visual stimuli were projected onto a vertical screen with a 23 × 30 degree visual angle placed inside the magnet bore using a MR-compatible Hyperion digital projection system (Psychology Software Tools, Pittsburgh, PA) placed at the back of the magnet room, and the stimulation presentation was controlled by a PC equipped with E-Prime (Psychology Software Tools, Pittsburgh, PA). The participants viewed the screen through a mirror mounted on top of the head coil. For the participants who needed vision correction, MR-compatible lenses were used. Head movement was minimized by restraint using tape and cushions. Each subject had four consecutive 12-min rs-fMRI scans under four conditions: (1) eyes fixated on a dim gray fixation mark at the screen center with a black background; (2) and (3) visual

Flow Chart of the Functional Scans

Figure 1.

Illustration of the sequence of the five functional scans. Pre-VS: prior to the 25-min visual stimulation; Post-VS: after the 25-min visual stimulation; and VCA: visual cortical activation. The 1-min gap between the second and third scan was used to prepare and start the latter scan. The only difference between Experiments I and II is that, during the 25-min visual stimulation, the stressful pattern was used in the former and the non-stressful pattern was used in the latter, respectively.

stimulation with alternating 2-sec stimulation on-and-off for 25 min; and (4) same as (1). To localize V1, each subject also had a functional localizer scan (200 sec) with the visual cortical activation paradigm. Figure 1 illustrates the flow chart of these five functional scans. Then, high-resolution isotropic (1 mm^3) T1-weighted volumetric images were obtained to cover the whole brain. These images were acquired with an inversion recovery fast spoiled gradient-recalled sequence. The timing of the inversion recovery was optimized to suppress the cerebrospinal fluid (CSF) signal.

Generation of Visual Cortical Activation Maps

The EPI images from the functional localizer scan were processed with AFNI [Cox, 1996] to yield the stimulation-induced activation maps. The "afni_proc.py" routine in AFNI was used to generate the scripts to process the fMRI data. For each subject, any signal spikes in the signal intensity time courses were first detected and removed. The acquisition timing difference was then corrected for different slice locations. The functional images were aligned to T1-weighted high-resolution volumetric images. With the last functional image as the reference, rigid-body motion correction was done in three translational and three rotational directions. The amounts of motion were estimated and these estimations were modeled in data analysis. For each subject, spatial blurring with a full width half maximum of 4 mm was used to reduce random noise. Finally, to generate the statistical activation maps, at each voxel, regression analysis was performed with the "3dDeconvolve" routine in AFNI [Cox, 1996] against the time course of the visual stimulation paradigm described earlier. In this regression analysis, a gamma function was modeled as the hemodynamic response function; the motion parameters estimated earlier, and the baseline, system-induced signal trends up to second degree of polynomial were also modeled.

Visual Cortical V1 Seed Selection

Our main goal is to investigate the effects of stressful visual stimulation on visual cortical FC. Based on the visual cortical activation maps and the calcarine sulcus, on each hemisphere, a spherical seed region with a radius of 4 mm was placed to the center of the maximally activated V1 area (i.e., the area with the maximal activation induced by the visual stimulus). To reduce bias caused by the potential difference in the two seeds on the two hemispheres, each of the two seeds was used to generate a FC map, and these two maps were compared to finely adjust the seed positions if necessary to generate a similar FC map for both seeds. Finally, the left and right seeds were combined together to form a V1 seed for each subject. This combined V1 seed was used to generate a visual cortical FC for each of the four RS conditions for each subject.

Rs-fMRI Data Analysis

Overall, the rs-fMRI correlation analysis was conducted using AFNI software with the V1 seed defined above [Fox et al., 2005; Zhu and Majumdar, 2014]. Before the performance of correlation analyses, pre-processing of the rs-fMRI time course was needed. The "afni_proc.py" routine in AFNI was used to generate the scripts to pre-process the rs-fMRI data. For each subject, any signal spikes in the signal intensity time courses were first detected and removed. The data points with excess motion (normalized motion derivative > 0.3 or voxel outliers > 10%) were identified and were modeled in analysis. The acquisition timing difference was then corrected for different slice locations. The functional images were aligned to T1-weighted high-resolution volumetric images. With the third functional image as the reference, rigid-body motion correction was done in three translational and three rotational directions. The amounts of motion and motion derivatives were estimated and these estimations were modeled in data analysis. For each subject, spatial blurring with a full width half maximum of 4 mm was used to reduce random noise, and also to reduce effects of inter-subject anatomical variation and Talairach transformation variation [Talairach and Tournoux, 1988] during group analysis. At each voxel, using the "3dDeconvolve" routine in AFNI [Cox, 1996], the potentially motion-introduced artifacts estimated earlier, data points found with excess motion, and the baseline, system-induced signal trends up to fifth degree of polynomial were modeled, and then were removed from the time course. The mean signal time courses at the CSF and the white matter were also modeled as nuisance signals. These signals were also removed from the time course with the "3dDeconvolve" routine. A band-pass filter with a range of 0.009 Hz – 0.08 Hz was also applied in the "3dDeconvolve" routine [Fox et al., 2005]. The final pre-processed time courses at all brain region voxels were then utilized in correlation analyses. For individual-subject analyses, with the "3dfim+" routine

in AFNI, correlation analyses were performed on every voxel of the brain against the time course of the average signal within the V1 seed region to produce a FC map for each of the four RS conditions. The correlation coefficient, that is, the R value, between a voxel's time course and the mean V1 seed time course quantifies the strength of FC between this voxel and the V1 seed. To prepare for group analysis, the R values were converted to Z values through Fisher's Z transformation to improve the normality of the distribution.

Region-of-Interest Analysis

Region-of-interest (ROI) analyses were performed in native space. For each of the four RS conditions, to test the potential effect of significance levels on the analysis and to enhance our confidence on the findings, six FC maps were computed at six levels of significance: (1) $P = 1.0 \times 10^{-5}$; (2) $P = 1.0 \times 10^{-6}$; (3) $P = 1.0 \times 10^{-7}$; (4) $P = 1.0 \times 10^{-8}$; (5) $P = 1.0 \times 10^{-9}$; and (6) $P = 1.0 \times 10^{-10}$. For each significance level, the four FC maps were first used to determine an overlapped ROI mask in the visual cortex across all the four RS conditions, and then the mask was used to obtain a ROI-mean R value for each RS condition. Then, for each of the six P-values and each subject group, the group-mean of the ROI-mean R values of the 12 subjects was computed and analyzed to investigate the visual stimulation effect of stressful or non-stressful striped patterns on the FC in the visual cortex, respectively.

Whole-Brain Group Analysis

Whole-brain group analyses were performed in ICBM 452 T1 atlas. In whole-brain group analyses, for each subject group, the correlation maps of all 12 subjects were warped to the ICBM 452 template. Whole-brain ANOVAs were conducted to compare the Z values between different RS conditions with a mixed-effect two-factor model. The visual stimulus condition was the first factor and was modeled as a fixed effect. Subject was the second factor and was modeled as a random effect. The ANOVAs were conducted with the "3dANOVA2" program in AFNI [Cox, 1996].

Multiple Comparison Correction for Whole-Brain Group Analysis on rs-fMRI

Cluster significances of the whole-brain ANOVAs, described above, were corrected for multiple comparisons using Monte Carlo simulation. First, the spatial smoothness of the image data was estimated using "3dFWHMx" in AFNI [Cox, 1996]. A cluster analysis with the "AlphaSim" software in AFNI was then used to estimate the overall statistical significance with respect to the whole brain. Based on the simulations, a cluster's connectivity was considered significant only if it was within a 1,240 mm^3 cluster in which

TABLE I. Group-mean values of ROI size and ROI-mean FC at the two significance levels for stressful and non-stressful striped patterns

Pattern	R	P	ROI size ($\mu \pm \sigma$) (cm^3)	ROI-mean FC ($\mu \pm \sigma$) (R)			
				Pre-VS	First VS	Second VS	Post-VS
Stressful	0.2582	1.0×10^{-5}	43.8 ± 31.4	0.51 ± 0.05	0.56 ± 0.06	0.59 ± 0.06	0.58 ± 0.05
Non-stressful	0.2582	1.0×10^{-5}	62.5 ± 21.2	0.55 ± 0.06	0.60 ± 0.04	0.55 ± 0.04	0.57 ± 0.06
Stressful	0.3715	1.0×10^{-10}	25.1 ± 20.1	0.60 ± 0.05	0.65 ± 0.05	0.68 ± 0.07	0.66 ± 0.04
Non-stressful	0.3715	1.0×10^{-10}	37.2 ± 13.7	0.62 ± 0.05	0.68 ± 0.04	0.63 ± 0.04	0.64 ± 0.06

Pre-VS: prior to the visual stimulation; first VS: the first half of the 25-min stimulation; second VS: the second half of the stimulation; Post-VS: after the stimulation; R: correlation coefficient; $\mu \pm \sigma$: mean ± standard deviation.

the voxels were contiguous and each had a voxel-based correlation with the seed corresponding to an uncorrected $P \leq 0.005$, achieving an effective whole-brain corrected $P \leq 0.046$.

RESULTS

Similarity of FC Maps between the Left and Right Hemisphere

Two FC maps were produced with the left and right V1 seed, respectively, and visually examined to check the similarity between these two FC maps. They were compared to finely adjust the seed positions if necessary to generate a similar FC map for both seeds, and the final two maps were similar in the visual cortex for each subject. This similarity demonstrates that the visual cortex was functionally well connected between the two hemispheres. The FC map generated with the combined V1 seed was similar as the two FC maps produced with the left and right V1 seeds, and was subsequently used for the ROI analysis to examine the visual stimulation effects of stressful versus non-stressful striped patterns on the visual cortical FC.

ROI Analysis

For each Exp, an overlapped ROI mask in the visual cortex across all the four RS conditions was first obtained for each of the six significance levels and each subject. As expected, the size of the ROI mask in the visual cortex varied with the significance level; the higher the significance level, the smaller the mask size (Table I). Similar results were obtained from all the six significance levels, demonstrating the independence of the results from the chosen significance level. For simplicity, we only present the results from the lowest and highest two significance levels. For the lowest significance level of $P = 1.0 \times 10^{-5}$, the group-mean mask size was 43.8 ± 31.4 cm^3 for Exp I and 62.5 ± 21.2 cm^3 for Exp II, respectively. Although the mean mask size of the latter is larger than that of the former, they are not significantly different from each other (two-tail t-test, $P = 0.10$, degrees of freedom [DOF] = 22). The mask size also showed a large inter-subject variation as

reflected in the large standard deviations. For the highest significance level of $P = 1.0 \times 10^{-10}$, the group-mean mask size was 25.1 ± 20.1 cm^3 for Exp I and 37.2 ± 13.7 cm^3 for Exp II, respectively, and they are also not significantly different from each other (two-tail t-test, $P = 0.10$, DOF = 22).

For the baseline RS condition prior to the visual stimulation with the significance level of $P = 1.0 \times 10^{-5}$, the R value of the mask ranged from 0.419 to 0.585 with group-mean 0.510 ± 0.047 for Exp I and from 0.494 to 0.658 with group-mean 0.550 ± 0.061 for Exp II, respectively (Table I). Although the group-mean R value of the latter is larger than that of the former, they are not significantly different from each other (two-tail t-test, $P = 0.09$, DOF = 22). For the significance level of $P = 1.0 \times 10^{-10}$, the R value of the mask ranged from 0.533 to 0.661 with group-mean 0.596 ± 0.045 for Exp I and from 0.568 to 0.711 with group-mean 0.625 ± 0.048 for Exp II, respectively. Again, these two group-mean R values are also not significantly different from each other (two-tail t-test, $P = 0.15$, DOF = 22), although the latter is larger than the former. For each significance level, to reduce inter-subject and inter-study variations, each ROI-mean R value of the four RS conditions was normalized by dividing it with the baseline ROI-mean R value for each subject, enabling comparisons: (1) between Exps I and II and (2) between the two significance levels.

The visual stimulation effects of the stressful versus non-stressful striped patterns on the FC in the visual cortex are illustrated in Figure 2. Comparing the RS condition of the first half of the 25-min visual stimulation with that of the baseline prior to the stimulation, the ROI-mean R value was significantly increased (two-tail paired t-test, maximal $P = 0.0077$, DOF = 11), regardless of the stressful or non-stressful stimulation and of the significance levels (Fig. 3A). The degree of this enhancement was about the same for both stressful and non-stressful stimulation with both significance levels. Comparing the RS condition of the second half of the stimulation with that of the first half, the ROI-mean R value continued to increase for the stressful stimulation. In contrary to this continued enhancement, the ROI-mean R value was reduced back to the baseline R value for the non-stressful stimulation (Fig. 3A), regardless of the significance levels, showing a significantly contrary effect between the stressful and non-
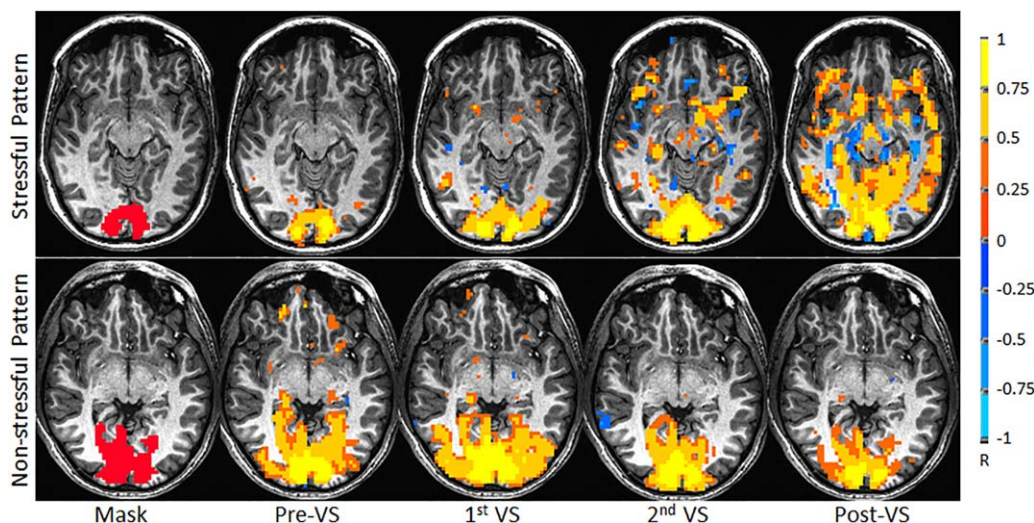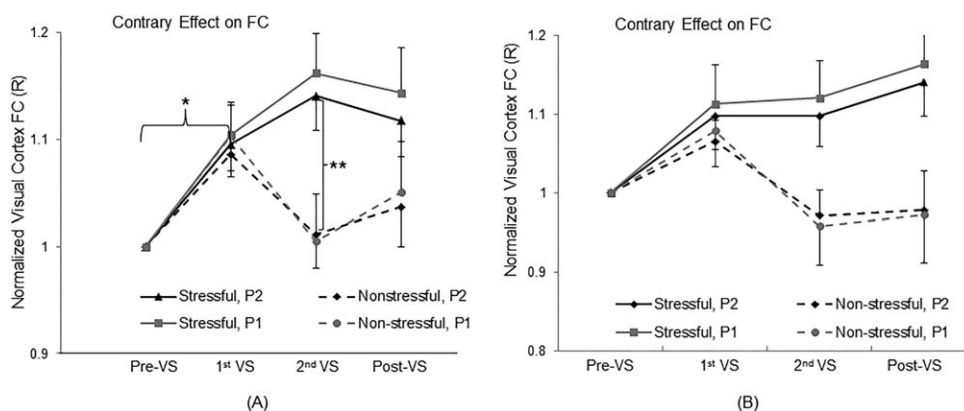
Figure 2.

Illustration of visual stimulation-enhanced functional connectivity in visual cortex for one representative subject ($R = 0.3315$, $P = 1.0 \times 10^{-8}$). From left to right: the overlapped ROI mask in the visual cortex, the baseline FC map prior to the visual stimulation (Pre-VS), the first FC map during the first half of the 25-min stimulation (first VS), the second FC map during the second half of the stimulation (second VS), and finally the FC map after the stimulation (Post-VS).

stressful striped patterns (two-tail t-test, maximal $P = 0.012$, DOF = 22). For the non-stressful stimulation, after the cessation of the stimulation, the visual cortical FC showed a larger but not significant R value than that in the baseline (two-tail paired t-test, minimal $P = 0.31$, DOF = 11), regardless of the significance levels. For the stressful stimulation, however, after the cessation of the stimulation, the visual cortical FC remained significantly larger than that in the baseline for both significance levels (two-tail paired t-test, maximal $P = 0.0062$, DOF = 11), demonstrating a lasting enhancement effect. Although the visual cortical FC after the stressful visual stimulation is substantially larger than that after the non-stressful visual stimulation (Fig. 3A, post-VS condition), the difference does not reach the statistically significant level of 0.05 (one-tail t-test, minimal $P = 0.061$, DOF = 22).

Figure 3.

Contrary effect of the stressful versus non-stressful striped patterns on the FC in the visual cortex during the second half of the 25-min visual stimulation. The vertical axis shows the normalized FC relative to that of the baseline. (**A**): Data from all subjects; and (**B**): Data from the six subjects who participated in both Experiments I and II. R: correlation coefficient; $P_1 = 1.0 \times 10^{-5}$; $P_2 = 1.0 \times 10^{-10}$; *: max $P = 0.0077$ (paired t-test, a total of four tests for the two experiments with two significance levels); **: max $P = 0.012$ (two-tails t-test, Experiment I vs. II, a total of two tests for the two significance levels); and error bar indicates the standard error of the means.
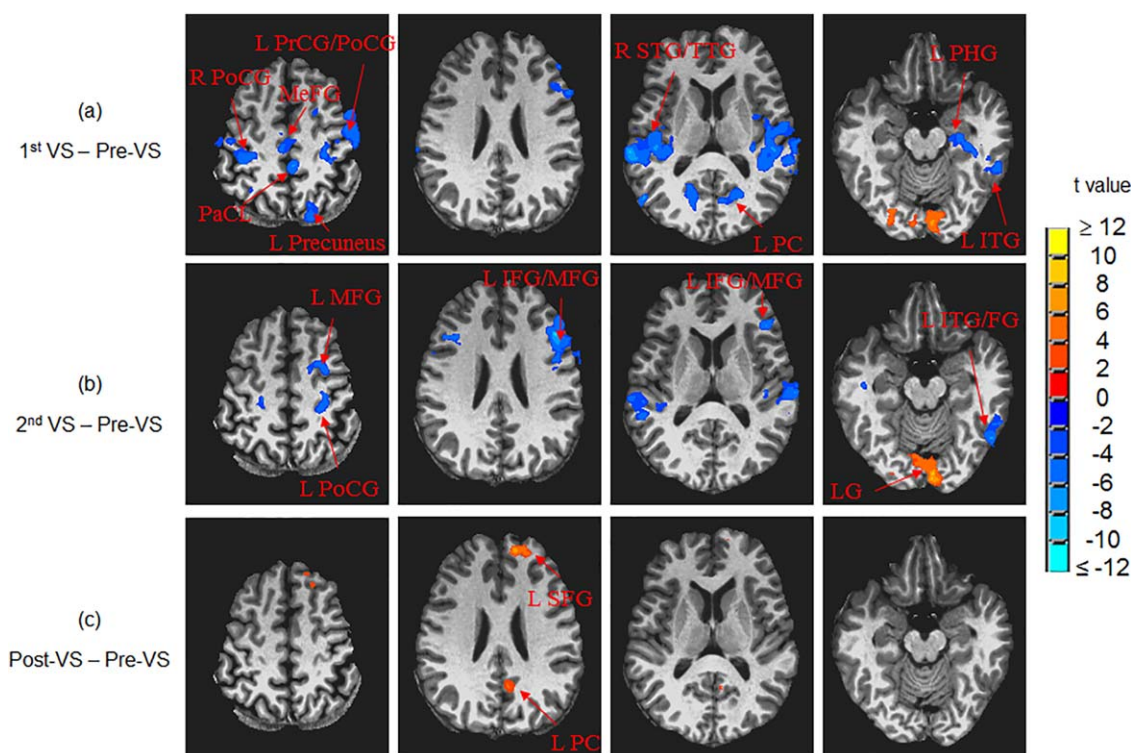
Figure 4.

Whole-brain ANOVAs showed significantly modified functional connectivity between V1 and other brain regions (comparing to the baseline prior to the visual stimulation): (**A**) during the first half of the 25-min stressful visual stimulation, (**B**) during the second half of the 25-min stressful visual stimulation, and (**C**) right after the stressful visual stimulation. R: right; L: left; PrCG: precentral gyrus; PoCG: postcentral gyrus; PaCL: paracentral lobule; IFG: inferior frontal gyrus; MFG: middle frontal gyrus; SFG: superior frontal gyrus; MeFG: medial frontal gyrus; ITG: inferior temporal gyrus; STG: superior temporal gyrus; TTG: transverse temporal gyrus; PC: posterior cingulate; LG: lingual gyrus; PHG: parahippocampal gyrus; FG: fusiform gyrus.

Whole-Brain Group Analysis

The whole-brain ANOVAs found significantly modified functional connectivity from other brain regions to V1 (comparing to baseline) during and after the 25-min stressful visual stimulation (Fig. 4). Besides the significant change on the visual cortex described above, the other notable regions were right and left precentral and postcentral gyri, right and left middle frontal gyri, right and left superior temporal gyri, and left inferior temporal gyrus. All these regions show changes from positive R values at baseline to nearly zero or negative R values. We wish to emphasize the results of ANOVAs that compare pre- and post-stimulation: left inferior frontal gyrus (L IFG), let superior frontal gyrus (L SFG), and left posterior cingulate cortex (L PCC) were significantly more connected to V1 after the cessation of the 25-min stressful visual stimulation (Fig. 5 and Table II), compared to before this visual stimulation. Before the stressful stimulation was applied, the R values between V1 and these clusters were nearly zero. The R values at these clusters were significantly increased after cessation of the 25-min stressful visual

stimulation (Table II). On the contrary, the whole-brain ANOVAs of this study did not find significant FC changes to V1 comparing before and after the application of the non-stressful stimulation.

DISCUSSION AND CONCLUSIONS

The effects of the visual stimulation from stressful versus non-stressful striped patterns on the visual cortical FC were tested with the ROI analysis. The analysis showed that the visual cortical FC was significantly increased during the first half of the 25-min visual stimulation in comparison to the baseline (Fig. 3A). This enhancement was independent of the stressfulness of the patterns, suggesting it was the basic visual stimulation but not the striped patterns that was mainly responsible for the enhancement during the early phase of the visual stimulation. For the non-stressful stimulation, the visual cortical FC returned back to the baseline level during the second half of the stimulation and remained at that level after the cessation
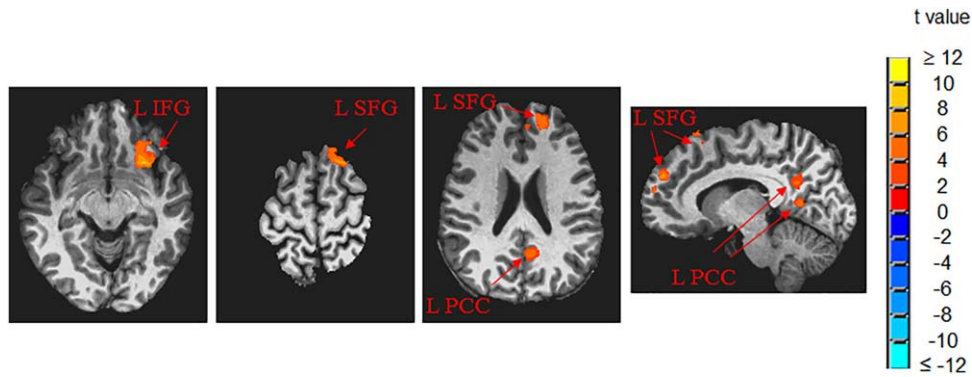
Figure 5.

Left inferior frontal gyrus (L IFG), let superior frontal gyrus (L SFG), and left posterior cingulate cortex (L PCC) were found to be significantly more connected to V1 after the 25-min stressful visual stimulation.

of the stimulation, suggesting a quick adaptation of the visual cortex to the non-stressful stimulation. For the stressful stimulation, however, the visual cortical FC continued to increase during the second half of the stimulation, suggesting an additional enhancement effect of the stimulation on the visual cortical FC that was most likely due to the stressful striped pattern. Furthermore, after the cessation of the stressful stimulation, although the visual cortex FC started to decline as expected, it remained significantly larger than that in the baseline, showing a lasting enhancement effect. As shown in Figure 3A, the similar FC behaviors were observed for both significance levels of 1.0×10^{-5} and 1.0×10^{-10}, showing the independence of these behaviors to the selection of the significance level. After the 25-min visual stimulation, although the difference between non-stressful and stressful stripes does not reach the statistically significant level of 0.05, the corresponding P-value is relatively small ($P = 0.061$), and the visual cortical FC after the stressful visual stimulation is substantially larger than that after the non-stressful stimulation at the post-VS condition, as shown in Figure 3A. In addition, contrary to non-stressful stripe that showed no significant difference between the pre- and post-VS conditions, stressful stripe showed a significant difference ($P = 0.0062$). Although

this one-time visual stressful stimulation-induced effect was acute and relatively short-lived, a repeated stimulation may induce a long-lasting effect.

The dramatically different histograms of the optimal SFs distribution for V1 neurons and V2 neurons might be responsible for the contrary effect of the stressful versus non-stressful striped patterns on the visual cortical FC (Fig. 3A). Accordingly, it would be very helpful to investigate both activation and FC changes in V1 and V2 in response to the stressful and non-stressful patterns for understanding the underlying mechanisms, but this investigation requires a highly accurate functional segmentation of V1 and V2 on each subject. Although V1 and V2 have their own functions, they are functionally connected. Segmentation with anatomy-based atlas likely leads to some overlapping functional regions between V1 and V2, and is thus not accurate enough for such an investigation. To the best of our knowledge, retinotopic mapping is the only technique that can provide reliably delineated V1 and V2 on each individual subject. In this pilot study, however, we did not acquire fMRI data for retinotopic mapping, and therefore did not investigate the different effects of the stressful versus non-stressful striped visual patterns on the functional connectivity to V1 and V2.

TABLE II. The increase of functional connectivity to V1 after the 25-min stressful visual stimulation

Cluster region	Size (mm³)	Centroid position in Talairach	t value (mean ± SEM)	Mean correlation r	
				Before stimulation	After stimulation
L SFG	2167	(L16, A53, S24)	4.44 ± 0.02	0.008	0.182
L IFG	1969	(L28, A24, I9)	4.66 ± 0.02	0.033	0.233
L SFG	1626	(L17, A25, S60)	4.32 ± 0.02	0.005	0.141
L PCC	1544	(L9, P55, S18)	3.84 ± 0.01	0.049	0.245

Abbreviations: R = right, L = left, A = anterior, P = posterior, I = inferior, S = superior, SEM = standard error of mean, SFG = superior frontal gyrus, IFG = inferior frontal gyrus, PCC = posterior cingulate cortex.

The lasting enhancement effect after the stressful stimulation went beyond visual cortex. The FCs between V1 and left IFG, SFG, and PCC were significantly increased (Table II and Fig. 5). These significant clusters are nicely mapped to the default-mode network (DMN) subnetworks as described by Yeo et al. [2011]. Specifically, the left inferior frontal gyrus (IFG) cluster maps to the node at the left ventral prefrontal cortex of the DMN subnetwork B; the more superior cluster found at the L SFG maps to the node at the left dorsal prefrontal cortex (PFCd) of the DMN subnetwork A, and the more inferior cluster found at the left SFG maps to the node at the left medial prefrontal cortex (PFCm) of DMN subnetwork A. The left PCC cluster maps to the node at the DMN subnetwork A. Prior studies largely supported the theory that DMN directly supports internal mentation that is largely detached from the external world [Buckner et al., 2008]. The DMN plays an important role in constructing dynamic mental simulation based on personal experience. In this role, the DMN is coupled to memory systems but not sensory systems. This role is consistent with our data that V1 was only weakly connected to DMN regions before the application of stressful visual stimulation. Interestingly, the V1 FCs to DMN regions significantly increased after the application of stressful stimulation. This enhanced connection between DMN and a sensory system suggests that the DMN can also play a role in monitoring the external environment when a demand is present. This DMN role was originally hypothesized by multiple groups [Gilbert et al., 2007; Hahn et al., 2007; Shulman et al., 1997] and later discussed in the review paper by Buckner et al. [2008] as one possible function. In sum, the possible DMN role in monitoring external environment appears to be in-line with our finding that the 25-min of the stressful visual stimulation enhanced the FC between the DMN and the visual cortex. Contrary to the non-stressful stimulation, the brain could not adapt to the stressful stimulation, and the accumulation of the DMN's continuous monitoring of the stressful pattern might be responsible for producing the enhanced FC between the DMN and the visual cortex. The functional connectivity between V1 and other brain regions appeared quite dynamic during and after stressful visual stimulation (Fig. 4), reflecting the initial exposure to the stressful stimulation during the first half of the 25-min visual stressful stimulation, and then the potential adaptation stage during the second half of stimulation, and the effect after the removal of the stimulation.

The alternating 2-sec stimulation on-and-off of the 25-min visual stimulation would induce a 0.25 Hz stimulus-modulated temporal signal pattern. This temporal signal pattern, however, should have no direct effect on the FC computation because that the signal time course was band-pass filtered to the range of 0.009 Hz – 0.08 Hz. Therefore, the stressful stimulation-enhanced FC across the visual cortex was due to the striped pattern of the visual stimulation, not the direct visual response to the on-off visual stimulation temporal pattern as in typical fMRI studies. The lasting enhancement effect on the FC after the cessation of the stressful stimulation provides a further evidence of this interpretation. This interpretation is also supported by the contrary effect of the non-stressful striped pattern on the visual cortical FC as shown in Figure 3A.

Neuromodulation approaches have been developed and tested for chronic headache treatment with electrical or magnetic stimulation of superficial and deep brain, occipital nerve, vagus nerve, sphenopalatine ganglion (SPG), and spinal cord [Martelletti et al., 2013]. Although the theoretical mechanisms may vary depending on the location and type of stimulation, almost all of these therapies require weeks to months of stimulation for a prophylactic effect to occur, suggesting neuronal plasticity as a possible mechanism [Martelletti et al., 2013]. The treatment effect may also depend on stimulation conditions as evidenced in the observations that low-frequency (LF) SPG stimulation provokes headache attacks while high-frequency (HF) SPG stimulation treats the attacks [Schytz et al., 2013], and LF repetitive transcranial magnetic stimulation (rTMS) reduces cortical excitability while HF rTMS increases it [Martens et al., 2013; Thickbroom, 2007]. This clearly illustrates the dependence of prophylactic treatment on specific stimulation conditions. For this reason, it is important to investigate the cortical response and search for specific modulating conditions. Because the difficulty of applying these electrical or magnetic stimulation techniques in an MRI environment, fMRI has rarely been used to investigate the cortical response in these settings. Our findings in this study suggest a potential new avenue of non-invasive treatment and monitoring of chronic headache.

The 25-min visual stimulation with the physiologically strong striped pattern, i.e., SF 2.8 cpd, significantly enhanced the FC within the visual cortex and altered the FC to V1 in other regions too, with a lasting effect even after the cessation of the stimulation. This suggests prolonged visual stimulation with the stressful pattern may alter visual system FC network and its relationship with other networks. Viewing this stressful pattern for a few seconds induces perceptual illusions and visual discomfort, and prolonged viewing without interruption may trigger headaches in patients with migraine and induce seizures in patients with photosensitive epilepsy [Wilkins, 1995]. The perception of these visual symptoms, however, diminishes with decreased SF, and the symptoms completely vanish when viewing the non-stressful striped pattern with SF 0.27 cpd, suggesting a transition function of the pattern-induced perceptual illusions with SF. The threshold SF_{TH}, above which the pattern provokes illusions, can be determined from the transition function, and then an appropriately selected supra-threshold SF, that is just above SF_{TH}, may be used to construct a safe, comfortable and repetitive visual stimulation paradigm to modulate visual cortical FC for prophylactic treatment in patients suffering visually triggered headaches or seizures. We hypothesize that, with a daily prolonged comfortable

visual stimulation, the brain will be gradually adapted to the stimulation and the adaptation consequently reduces the visual cortical hyper-response to the stimulation. If this hypothesis is correct, then the adaptation should yield a new transition function with a decreased number of the perceptual illusions induced by the SF. After the brain is adapted to the first selected SF, the new transition function can be used to appropriately select a second slightly increased SF to repeat the whole visual modulation process, and the consequent adaptation would further reduce the visual cortical hyper-response. Repeating this process with successively increased SFs until the brain is adapted to all SFs may result in a modulation-reduced visual cortical hyper-response to the stressful patterns. Such a study, however, is beyond the scope of this study.

The main goal of this study was to test the effects of stressful visual stimulation on visual cortical FC. To the best of our knowledge, this is the very first rs-fMRI study to investigate these effects. This is our first pilot study to investigate the dynamic change of the brain connectivity under and after visual stressful stimulation. The one-time visual stressful stimulation-induced effect was acute and relatively short-lived. Based on the time course of the visual cortex functional connectivity (Fig. 3A), we estimate that it would take 0.5–1 h to recover back to the baseline before the visual stimulation was applied. It will be interesting to find out how long the effect lasts and whether repeated application of this visual stressful simulation will alter the length of the recovery. These questions are important because they are directly related to the potential of using visual stimulation as a tool in the treatment of migraine headaches and seizures. Interestingly, Forster and his colleagues demonstrated that a seizure patient with a sensitive range from 15 to 35 Hz was rendered insensitive to the 20 Hz visual stimulation after repeated administration of visual stimulation at this frequency, but seizure discharges were still produced at the frequencies of 15, 25, or 30 Hz [Forster et al., 1964]. This implies a frequency-specific adaptation to repeated visual stimulation and potentially lasting effect.

In summary, in addition to the pattern-induced perceptual illusions/distortions and visual discomfort in most people, headaches in patients with migraine, and seizures in patients with photosensitive epilepsy, the stressful striped pattern with SF 2.8 cpd was found to provoke an enhancing and lasting effect on the visual cortical FC. The visual cortical hyper-response to this stressful pattern is likely to be responsible for these pattern-induced symptoms. In contrary, the non-stressful striped pattern with SF 0.27 cpd did not induce any such effects. These results suggest that an appropriately selected SF may be used to construct a safe, comfortable and repetitive stimulation paradigm to visually modulate the visual cortical hyper-response, and a modulation-reduced visual cortical hyper-response may yield a non-invasive neuromodulation technique for prophylactic treatment of visually triggered headaches and seizures.

REFERENCES

Biswal B, Yetkin FZ, Haughton VM, Hyde JS (1995): Functional connectivity in the motor cortex of resting human brain using echo-planar MRI. Magn Reson Med 34:537–541.

Buckner RL, Andrews-Hanna JR, Schacter DL (2008): The brain's default network: Anatomy, function, and relevance to disease. Ann N Y Acad Sci 1124:1–38.

Campbell FW, Robson JG (1968): Application of Fourier analysis to the visibility of gratings. J Physiol 197:551–566.

Cao Y, Welch KM, Aurora S, Vikingstad EM (1999): Functional MRI-BOLD of visually triggered headache in patients with migraine. Arch Neurol 56:548–554.

Cao Y, Aurora SK, Nagesh V, Patel SC, Welch KM (2002): Functional MRI-BOLD of brainstem structures during visually triggered migraine. Neurology 59:72–78.

Cox RW (1996): AFNI: Software for analysis and visualization of functional magnetic resonance neuroimages. Comput Biomed Res 29:162–173.

Forster FM, Ptacek LJ, Peterson WG, Chun RW, Bengzon AR, Campos GB (1964): Stroboscopic-induced seizure discharges. Modification by extinction techniques. Arch Neurol 11:603–608.

Foster KH, Gaska JP, Nagler M, Pollen DA (1985): Spatial and temporal frequency selectivity of neurones in visual cortical areas V1 and V2 of the macaque monkey. J Physiol 365:331–363.

Fox MD, Snyder AZ, Vincent JL, Corbetta M, Van Essen DC, Raichle ME (2005): The human brain is intrinsically organized into dynamic, anticorrelated functional networks. Proc Natl Acad Sci USA 102:9673–9678.

Gilbert SJ, Dumontheil I, Simons JS, Frith CD, Burgess PW (2007): Comment on "Wandering minds: The default network and stimulus-independent thought". Science 317:43.

Hadjikhani N, Sanchez Del Rio M, Wu O, Schwartz D, Bakker D, Fischl B, Kwong KK, Cutrer FM, Rosen BR, Tootell RB, Sorensen AG, Moskowitz MA (2001): Mechanisms of migraine aura revealed by functional MRI in human visual cortex. Proc Natl Acad Sci USA 98:4687–4692.

Hahn B, Ross TJ, Stein EA (2007): Cingulate activation increases dynamically with response speed under stimulus unpredictability. Cereb Cortex 17:1664–1671.

Huang J, Cao Y (2012): Functional MRI as a biomarker for evaluation and prediction of effectiveness of migraine prophylaxis. Biomark Med 6:517–527.

Huang J, Cooper TG, Satana B, Kaufman DI, Cao Y (2003): Visual distortion provoked by a stimulus in migraine associated with hyperneuronal activity. Headache 43:664–671.

Huang J, Zong X, Wilkins A, Jenkins B, Bozoki A, Cao Y (2011): fMRI evidence that precision ophthalmic tints reduce cortical hyperactivation in migraine. Cephalalgia 31:925–936.

Hubel DH, Wiesel TN (1962): Receptive fields, binocular interaction and functional architecture in the cat's visual cortex. J Physiol 160:106–154.

Hubel DH, Wiesel TN (1968): Receptive fields and functional architecture of monkey striate cortex. J Physiol 195:215–243.

Kwong KK, Belliveau JW, Chesler DA, Goldberg IE, Weisskoff RM, Poncelet BP, Kennedy DN, Hoppel BE, Cohen MS, Turner R, Cheng H-M, Brady TJ, Rosen BR (1992): Dynamic magnetic resonance imaging of human brain activity during primary sensory stimulation. Proc Natl Acad Sci USA 89:5675–5679.

Logothetis NK (2008): What we can do and what we cannot do with fMRI. Nature 453:869–878.

Martelletti P, Jensen RH, Antal A, Arcioni R, Brighina F, de Tommaso M, Franzini A, Fontaine D, Heiland M, Jurgens TP, Leone M, Magis D, Paemeleire K, Palmisani S, Paulus W, May A (2013): Neuromodulation of chronic headaches: Position statement from the European Headache Federation. J Headache Pain 14:86.

Martens JW, Koehler PJ, Vijselaar J (2013): Magnetic flimmers: 'light in the electromagnetic darkness'. Brain 136:971–979.

Nulty DD, Wilkins AJ, Williams JM (1987): Mood, pattern sensitivity and headache: A longitudinal study. Psychol Med 17: 705–713.

Ogawa S, Lee TM, Kay AR, Tank DW (1990): Brain magnetic resonance imaging with contrast dependent on blood oxygenation. Proc Natl Acad Sci USA 87:9868–9872.

Schytz HW, Barlose M, Guo S, Selb J, Caparso A, Jensen R, Ashina M (2013): Experimental activation of the sphenopalatine ganglion provokes cluster-like attacks in humans. Cephalalgia 33:831–841.

Shulman GL, Fiez JA, Corbetta M, Buckner RL, Miezin FM, Raichle ME, Petersen SE (1997): Common blood flow changes across visual tasks: II. Decreases in cerebral cortex. J Cogn Neurosci 9:648–663.

Singh KD, Smith AT, Greenlee MW (2000): Spatiotemporal frequency and direction sensitivities of human visual areas measured using fMRI. Neuroimage 12:550–564.

Talairach J, Tournoux P (1988): Co-Planar Stereotaxic Atlas of the Human Brain: 3D Proportional System. New York: Thieme.

Thickbroom GW (2007): Transcranial magnetic stimulation and synaptic plasticity: Experimental framework and human models. Exp Brain Res 180:583–593.

Wilkins A (1995): Visual Stress. Oxford: Oxford University Press.

Wilkins A, Nimmo-Smith I, Tait A, McManus C, Della Sala S, Tilley A, Arnold K, Barrie M, Scott S (1984): A neurological basis for visual discomfort. Brain 107: 989–1017.

Wilkins A, Milroy R, Nimmo-Smith I, Wright A, Tyrrell R, Holland K, Martin J, Bald J, Yale S, Miles T, Noakes T (1992): Preliminary observations concerning treatment of visual discomfort and associated perceptual distortion. Ophthalmic Physiol Opt 12:257–263.

Wilkins AJ, Patel R, Adjamian P, Evans BJ (2002): Tinted spectacles and visually sensitive migraine. Cephalalgia 22:711–719.

Yeo BT, Krienen FM, Sepulcre J, Sabuncu MR, Lashkari D, Hollinshead M, Roffman JL, Smoller JW, Zollei L, Polimeni JR, Fischl B, Liu H, Buckner RL (2011): The organization of the human cerebral cortex estimated by intrinsic functional connectivity. J Neurophysiol 106:1125–1165.

Zhu DC, Majumdar S (2014): Integration of resting-state FMRI and diffusion-weighted MRI connectivity analyses of the human brain: Limitations and improvement. J Neuroimaging 24:176–186.